Optimal Guidance for Aerodynamically Controlled Re-Entry Vehicles

MIGUEL A. DE VIRGILIO*
Aerospace Corporation, El Segundo, Calif.

AND

GERALD R. WELLS† AND EARL E. SCHIRING†
Logicon, Inc., San Pedro, Calif.

Linear optimal control theory is applied to develop terminal guidance laws for aerodynamically controlled re-entry vehicles. The quadratic performance function minimized includes the terminal state error, the integral of the state deviation from the nominal trajectory, and the integral of control corrections, where the weighting coefficients are trajectory dependent parameters. The vehicle is assumed to be controlled by lift acceleration magnitude and bank angle. By use of linear regulator theory, perturbation feedback control gains are calculated and used with state errors to compute corrections to the commanded nominal lift acceleration and bank angle. A four-state perturbation model is used to approximate the six-state trajectory dynamics for the derivation of the guidance feedback gain matrix. The notable feature of the approach described in this paper stems from the elimination of the velocity magnitude state in the flight dynamics perturbation model. In addition, "time" is eliminated as the independent variable in favor of distance, resulting in a four-state perturbation model. With these and other assumptions, the control variables are lift acceleration and bank angle, which are the natural ones for an acceleration controlled vehicle using accelerometers for measurement. This unique approach to modeling avoids the need for consideration of angle of attack and aerodynamic drag in the guidance equations. The guidance law implementation is thus independent of vehicle parameters such as mass and surface area, atmospheric density, and the aerodynamic coefficients of lift and drag. The resulting guidance law is evaluated using a three-degree-of-freedom simulation, in which the angle of attack and accelerations are limited and the trajectory dynamics are described by a six-state set of differential equations. Good performance is obtained for a variety of initial state errors, and off-nominal conditions in atmospheric density and vehicle aerodynamic lift and drag coefficients.

Nomenclature

A^* = modified lift magnitude = $A_L/V^2(\text{ft}^{-1})$
A_L = lift acceleration, ft/sec^2
A_{COM} = commanded vehicle acceleration, ft/sec^2
C_{L_α} = aerodynamic lift coefficient slope, rad^{-1}
C_L = aerodynamic lift coefficient
C_D = aerodynamic drag coefficient
D = aerodynamic drag, lb
F = homogeneous matrix of linear perturbation equation, 4×4
g = gravitational acceleration, ft/sec^2
G = forcing matrix of linear perturbation equation, 4×2
J = performance index
K = guidance feedback gain matrix, 2×4
L = aerodynamic lift, lb
m = mass, slugs
P = solution of matrix Riccati equation, 4×4
P_f = weighting matrix on terminal state error, 4×4
Q = weighting matrix, on-route state error, 4×4
R = weighting matrix, on-route control error, 2×2
S = reference area, ft^2
t = time, sec
$\mathbf{u}$ = control vector, 2×1
V = velocity magnitude, fps
$\mathbf{x}$ = system state vector, 4×1
X = downrange distance, ft
Y = crossrange distance, ft
Z = altitude, ft
α = angle of attack, rad
γ = flight path angle, rad
δ = variation from nominal
ρ = atmospheric density, slugs/ft^3
ϕ = bank angle, rad
ψ = azimuth angle, rad
τ = dummy time variable, sec

Subscripts
o = initial
f = final
N = nominal
M = maximum allowable

Presented as Paper 73-891 at the AIAA Guidance and Control Conference, Key Biscayne, Fla., August 20–22, 1973; submitted September 11, 1973; revision received March 11, 1974. This work was funded by USAF Contract F04701-72-C-0030. Appreciation is acknowledged for the help and cooperation of D. C. Depree, SAMSO, and A. J. Witsmeer of the Boeing Corporation.

Index categories: LV/M Guidance Systems; LV/M Dynamics and Control; Navigation, Control, and Guidance Theory.

* Member of Technical Staff, Guidance and Control Division. Member AIAA.

† Member of Technical Staff, Systems Analysis Department.

Introduction

THERE has been much research reported on different guidance methods for maneuvering re-entry vehicles and the reference list includes only a few of those most pertinent to this paper.[1–3] The majority of the literature is concerned with the initial atmospheric re-entry where vehicle heating is the important concern. Some papers discuss the terminal phase of re-entry where it is important to guide a re-entry vehicle such as the space shuttle to a landing site within allowable position errors.

This paper considers the application of linear optimal guidance to re-entry vehicles of the ballistic missile class, wherein the vehicles have the general appearance of sharp-nosed slender conical bodies.‡ The initial re-entry velocity considered was

‡ Vehicle parameters and aerodynamic data for the evaluation of the guidance laws were similar to the example case used in an unclassified report, with unlimited distribution.[4]

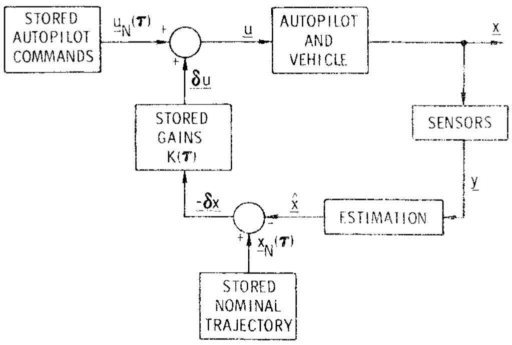

Fig. 1 Linear regulator guidance scheme.

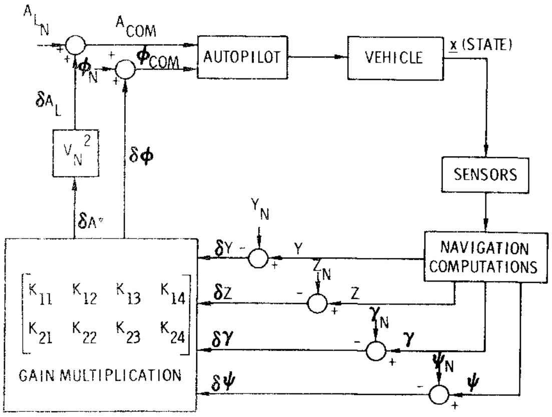

Fig. 2 Functional block diagram of linear regulator guidance mechanization.

hypersonic, and the vehicle experienced a wide dynamic pressure range. In addition, large lateral maneuvering capability was assumed in the definition of the various nominal re-entry trajectories that were used in the evaluation.

The majority of the literature pertinent to the terminal re-entry guidance problem uses angle of attack (α) and bank angle (ϕ) for the two control variables. If the nominal trajectory is defined using acceleration commands, the acceleration correction δA must be computed from the angle-of-attack correction using the equation

$$\delta A = \frac{1}{2}\frac{\rho(Z)V^2S}{m}C_{L_\alpha}\,\delta\alpha \tag{1}$$

This equation involves the vehicle nominal properties of mass m, reference area S, an inaccurate lift slope C_{L_α}, and also requires knowledge of atmospheric density, which is a function of the Z state variable. For off-nominal conditions on any combination of these parameters, an inaccurate δA feedback correction is demanded for angle-of-attack control. The perturbation dynamics model developed in this article is independent of these parameters, and does not use $\delta\alpha$ control.

Linear Regulator Technique

The linear optimal control theory results in a feedback law which computes corrections to the nominal commands, as shown in Fig. 1 in general. The perturbation equations are

$$\boldsymbol{\delta x}' = F\,\boldsymbol{\delta x} + G\,\boldsymbol{\delta u} \tag{2}$$

where "prime" denotes d/dX, and

$$\boldsymbol{\delta x} = \mathbf{x} - \mathbf{x}_N \tag{3}$$

$$\mathbf{u} = \mathbf{u}_N + \boldsymbol{\delta u} \tag{4}$$

The performance function minimized was the quadratic function J

$$J = \tfrac{1}{2}\boldsymbol{\delta x}_f{}^T P_f\,\boldsymbol{\delta x}_f + \tfrac{1}{2}\int_{X_o}^{X_f}\left[\boldsymbol{\delta x}^T Q\,\boldsymbol{\delta x} + \boldsymbol{\delta u}^T R\,\boldsymbol{\delta u}\right]dX \tag{5}$$

where P_f, Q, and R are weighting, or penalty matrices which must be selected by the designer. The matrix R must be positive definite, while Q and P_f need be positive semidefinite. These weighting matrices are usually symmetric and diagonal to minimize the number of parameters to choose.

Minimization of J in Eq. (5) produces the requirement to solve the matrix differential Riccati equation

$$P(X)' = -F^TP - PF + PGR^{-1}G^TP - Q \tag{6}$$

which is solved backward in X, starting from the terminal condition $P = P_f$ using the VASP[5] programs. The feedback gain matrix is then determined from

$$K = R^{-1}G^TP \tag{7}$$

and is X-varying throughout the trajectory. The control correction is then

$$\boldsymbol{\delta u} = -K\,\boldsymbol{\delta x} \tag{8}$$

The mechanization of the linear optimal guidance scheme is given in Fig. 2, which is the basic block diagram used in the 3-DOF simulation for the evaluation of the linear optimal guidance law.

Equations of Motion and Simplified Model

The coordinate system that was used was centered at the desired target, and was an orthogonal triad with Z positive upward along the local vertical, X pointing downrange, and Y completing the right-hand set. The wind axis coordinate frame was used for the point mass vehicle, and is shown in Fig. 3 for the equations:

$$\dot{X} = V\cos\gamma\cos\psi \tag{9}$$

$$\dot{Y} = -V\cos\gamma\sin\psi \tag{10}$$

$$\dot{Z} = V\sin\gamma \tag{11}$$

$$\dot{V} = -D/m - g\sin\gamma \tag{12}$$

$$\dot{\gamma} = \frac{L\cos\phi}{mV} - \frac{g\cos\gamma}{V} \tag{13}$$

$$\dot{\psi} = \frac{L\sin\phi}{mV\cos\gamma} \tag{14}$$

Reduction to the Four-State Model

At this point some of the system's accuracy requirements and vehicle's characteristics were used to reduce the dimension of the state vector. Deviations from the nominal magnitude of the velocity were the least stringent of the performance requirements. On the other hand, V is not a state over which control can be exerted directly (at least for small angles of attack); thus, the V state can be approximated as an uncontrollable one. These two facts indicated that the V state could be eliminated from the equation set and V_N be used wherever V was needed.

Another valid assumption was that the gravity force was negligible when compared to either the lift force L or the drag force D. The remaining equation set was transformed to use the

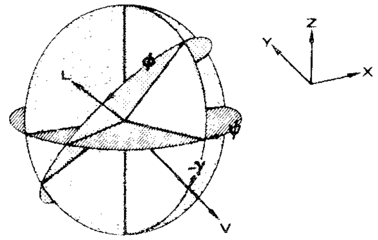

Fig. 3 Wind frame coordinate system.

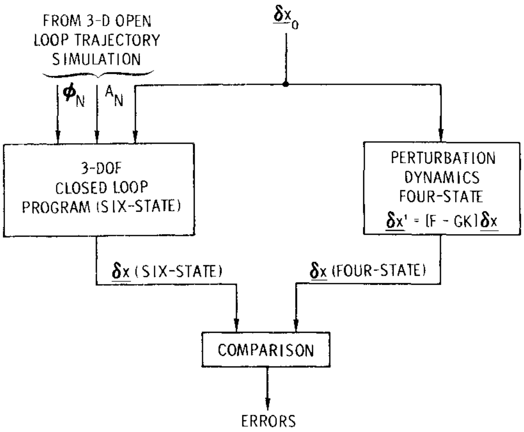

Fig. 4 Four-state perturbation dynamics model validation.

downrange variable X as the independent variable, eliminating time explicitly from the equations. The resulting equations are

$$dY/dX = -\tan\psi \tag{15}$$

$$dZ/dX = \tan\gamma/\cos\psi \tag{16}$$

$$d\gamma/dX = L\cos\phi/mV_N{}^2\cos\gamma\cos\psi \tag{17}$$

$$d\psi/dX = L\sin\phi/mV_N{}^2\cos^2\gamma\cos\psi \tag{18}$$

If the lift force is represented by the mass times the acceleration, $L = mA_L$, and if a modified acceleration A^* is defined as

$$A^* = A_L/V_N{}^2 \tag{19}$$

then the four-state trajectory dynamics equations for the feedback model are

$$dY/dX = -\tan\psi = f_1(\psi) \tag{20}$$

$$dZ/dX = \tan\gamma/\cos\psi = f_2(\gamma,\psi) \tag{21}$$

$$d\gamma/dX = A^*\cos\phi/\cos\gamma\cos\psi = f_3(\gamma,\psi,A^*,\phi) \tag{22}$$

$$d\psi/dX = A^*\sin\phi/\cos^2\gamma\cos\psi = f_4(\gamma,\psi,A^*,\phi) \tag{23}$$

Note the above equations are independent of all vehicle properties, density, aerodynamic coefficients, and angle of attack—they are functions of only the states γ, ψ and the control inputs A^*, ϕ.

Perturbation Dynamics Equations

The four-state linearized equations of motion are obtained by taking first-order perturbations about a nominal trajectory. The form of the perturbation equation is

$$\underbrace{\frac{d}{dX}\begin{bmatrix}\delta Y\\ \delta Z\\ \delta\gamma\\ \delta\psi\end{bmatrix}}_{\delta \mathbf{x}'} = \underbrace{\begin{bmatrix}0 & 0 & 0 & F_{14}\\ 0 & 0 & F_{23} & F_{24}\\ 0 & 0 & F_{33} & F_{34}\\ 0 & 0 & F_{43} & F_{44}\end{bmatrix}}_{F}\underbrace{\begin{bmatrix}\delta Y\\ \delta Z\\ \delta\gamma\\ \delta\psi\end{bmatrix}}_{\delta\mathbf{x}} + \underbrace{\begin{bmatrix}0 & 0\\ 0 & 0\\ G_{31} & G_{32}\\ G_{41} & G_{42}\end{bmatrix}}_{G}\underbrace{\begin{bmatrix}\delta A^*\\ \delta\phi\end{bmatrix}}_{\delta\mathbf{u}} \tag{24}$$

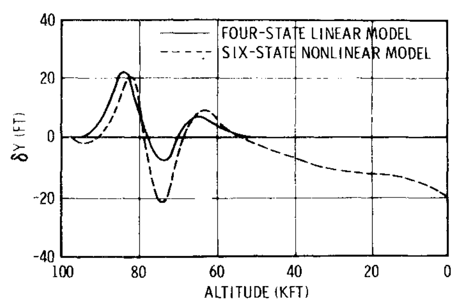

Fig. 5 Crossrange error comparison; four-state model validation; $\delta X_o = 1000$ ft.

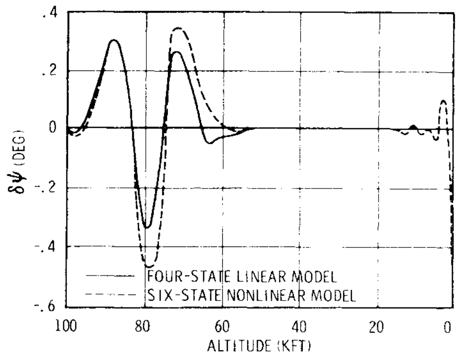

Fig. 6 Azimuth angle error comparison; four-state model validation; $\delta X_o = 1000$ ft.

where

$$F_{ij} = \partial f_i/\partial x_j;\quad G_{ij} = \partial f_i/\partial u_j$$

Perturbation Model Validation

The four-state model was validated according to the scheme shown on Fig. 4. Initial condition perturbations were applied to both the four-state linear model, and also the 3-DOF closed-loop six-state simulation using the guidance feedback gains determined from the four-state model. The 3-DOF simulation contained the nonlinear dynamics equations, Eqs. (9–14) with angle-of-attack limiting at high altitude. The hypothesis is that if the transient does not stray too far from the nominal, then the approximations given in the four-state model are valid.

Three comparisons between the nonlinear (six state) and linear (four state) transients due to an initial perturbation in X of 1000 ft are shown in Figs. 5–7 (this comparison was done with altitude as the independent variable). The difference in the terminal position is within 20 ft, and the difference in terminal azimuth angle is within 0.5°. Figure 7 shows the velocity magnitude perturbation caused by the initial transient in the nonlinear simulation. Since this state was neglected in the linear case, the six-state model is compared to the zero line on the plot. The result shows that the velocity perturbation is different from the nominal by 100 fps throughout the transient, where the initial re-entry velocity nominal magnitude is hypersonic.

In view of this four-state model comparison with the nonlinear six-state simulation, it was concluded that the four-state model is an adequate one for determining the linear optimal guidance gains.

Weighting Matrix Selection Process

The only design specification attainable using linear optimal control without trial and error work is the closed-loop system stability. Indeed, the linear optimal regulator theory guarantees stability if certain conditions on F, G, P_f, Q, and R are met.[3] Guidance requirements for re-entry vehicles may demand besides

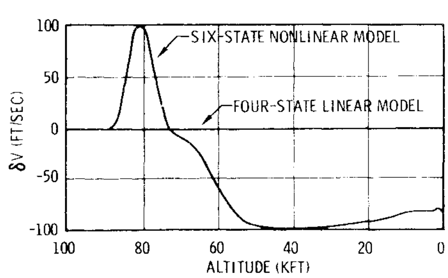

Fig. 7 Velocity error comparison; four-state model validation; $\delta X_o = 1000$ ft.

stability, a good nominal path following, and small terminal errors under a variety of perturbations and off-nominal conditions. The designer must be able to produce a set of weighting matrices P_f, Q, and R that satisfy those specifications. Some theoretical work has been done[6] in order to define analytically the weighting matrices, but is only restricted to time invariant plants. Since the re-entry guidance problem is inherently time varying, no direct application of these techniques was possible.

Rule-of-Thumb Choice

The rule of thumb mentioned in the literature[7] is to use the squares of the reciprocals of desired terminal accuracy values at the final time for P_f, and to use the squares of the reciprocals of maximum allowable deviations from the nominal variables throughout the trajectory for Q and R, as illustrated in Eqs. (25–27).

$$P_f = \begin{bmatrix} \frac{1}{\delta Y_f^2} & 0 & 0 & 0 \\ 0 & \frac{1}{\delta Z_f^2} & 0 & 0 \\ 0 & 0 & \frac{1}{\delta \gamma_f^2} & 0 \\ 0 & 0 & 0 & \frac{1}{\delta \psi_f^2} \end{bmatrix} \tag{25}$$

$$Q = \begin{bmatrix} \frac{1}{\delta Y_M^2} & 0 & 0 & 0 \\ 0 & \frac{1}{\delta Z_M^2} & 0 & 0 \\ 0 & 0 & \frac{1}{\delta \gamma_M^2} & 0 \\ 0 & 0 & 0 & \frac{1}{\delta \psi_M^2} \end{bmatrix} \tag{26}$$

$$R = \begin{bmatrix} \frac{1}{\delta A^*{}_M{}^2} & 0 \\ 0 & \frac{1}{\delta \phi_M^2} \end{bmatrix} \tag{27}$$

The rule-of-thumb selection method did produce acceptable results for a first guess, and was valuable in this regard. However, improvement in terminal errors was seen possible, especially for off-nominal perturbations. The standard linear regulator theory is intended to optimize the response to initial conditions rather than sustained atmospheric and aerodynamic off-nominal conditions. One technique for minimizing this type of sustained disturbance, is through the use of integral state feedback,[6,8] but at the expense of increasing the number of states. Because of the requirement for computational simplicity of the guidance law, the integral state feedback approach was not attempted.

Systematic Approach to P_f, Q, R, Selection

For lack of an analytical approach to the selection of P_f, Q, R, a systematic approach to the choice was followed as shown in Fig. 8. The initial guess used the "rule-of-thumb" approach described in the previous section. The resulting gains were used for initial condition transients within the linear optimal program. If the terminal errors were not essentially zero, then no further evaluation was done and P_f, Q, R were modified and re-evaluated in the linear optimal program.

If the linear transient performance was acceptable, then the nonlinear 3-DOF simulation was used for evaluation of the nominal trajectory. If the nonlinear nominal results were not acceptable, then P_f, Q, R were again modified and the linear optimal iteration loop was again used.

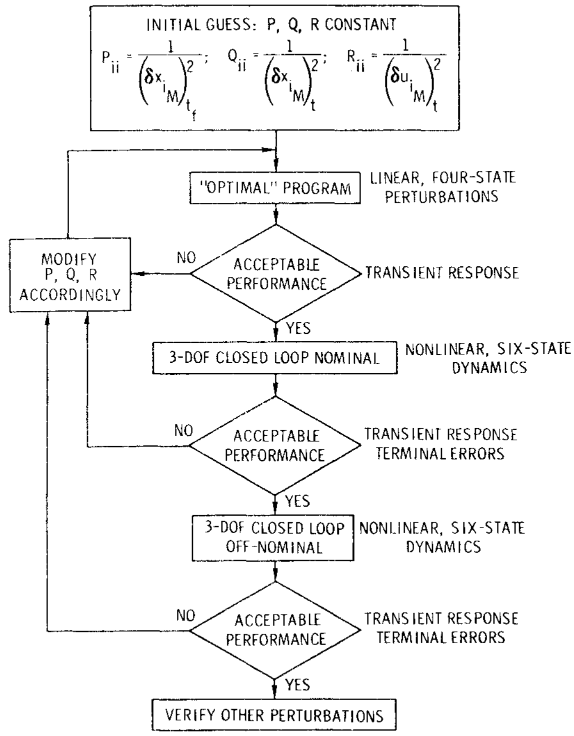

Fig. 8 Weighting matrix study flow diagram.

If the 3-DOF nonlinear simulation showed acceptable performance for the nominal trajectory, then further 3-DOF simulation evaluation was done for initial perturbations and off-nominal conditions. If these terminal errors were unacceptable, then P_f, Q, R were modified again and the whole process was repeated.

Weighting Matrix Iterations

In the preceding section, the orderly process that was used for evaluating R, Q, and P_f was outlined. The history of the actual modification is discussed next. An attempt is made to give a flavor for the sensitivity of the terminal errors to changes in R, Q, P_f. While other weighting matrix sets were used in arriving at the "best" one, only five sets are discussed. The "best" one, set 5, is certainly not a mathematical best, and some minor improvements could probably be made by additional trial and error, but set 5 resulted in such good terminal error performance that further attempts for improvement were not justified in a practical sense. The constituents of the weighting matrices are shown in Table 1. The discussion which follows is in order of observed importance of the weighting matrices, R, Q, P_f.

The R Matrix

An angle-of-attack restriction of $0° \leq \alpha \leq \alpha_M$ was placed on the vehicle. The lower limit of 0° was assumed as a vehicle restriction. Because of these limits in the 3-DOF nonlinear simulation, care was needed in the selection of the R matrix, in particular the R_{11} element in such a way as to place large penalties on commanded accelerations that would exceed the angle-of-attack limits. Thus, by suitable choice of R_{11}, the closed-loop performance was controlled to be nearly linear; i.e., small perturbations about the nominal trajectory. In addition since $R_{11} = (1/\delta A^*{}_M)^2$, and since δA_{L_M} was desired to have certain values throughout the trajectory, then $\delta A^* = \delta A_L / V^2$ was made variable using $V_N{}^2(X)$ for the particular trajectory. The resulting variable R_{11} elements are shown in Fig. 9.

The terminal errors for the $+10\%$ C_D off-nominal condition are shown in Table 2 for several different weighting matrix sets

Table 1 Weighting matrix set constituents

Constituent value		Set number 1	2	3	4	5
R	δA^*_M (ft^{-1})	Variable[a]	Variable[a]	Variable[a]	Variable[b]	Variable[b]
	$\delta\phi_M$ (deg)	10	10	10	10	10
Q	δY_M (ft)	1000	Variable 1000–10	1000	1000	Variable 1000–10
	δZ_M (ft)	1000	Variable 1000–10	1000	1000	Variable 1000–10
	$\delta\gamma_M$ (deg)	1	1	1	1	1
	$\delta\psi_M$ (deg)	1	1	1	1	1
P_f	δY_f (ft)	10	10	1	1	10
	δZ_f (ft)	10	10	1	1	10
	$\delta\gamma_f$ (deg)	1	1	0.1	0.1	1
	$\delta\psi_f$ (deg)	1	1	0.1	0.1	1

[a] R_{11} penalized for $\alpha \geqq \alpha_M$.
[b] R_{11} penalized for $\alpha \geqq \alpha_M$ and $\alpha \leqq 0°$.

Table 2 Terminal errors for $+10\%$ C_D off-nominal conditions

Weighting matrix set	ΔX_f (ft)	ΔY_f (ft)	$\Delta\gamma_f$ (deg)	$\Delta\psi_f$ (deg)	ΔMach$_f$	Δt_f (sec)
1	120	179	−0.3	−1.1	−0.95	0.86
2	−248	152	−2.9	3.2	−1.07	0.86
3	−80	112	1.4	0.3	−0.88	0.85
4	−2	37	−0.1	−0.4	−0.74	0.83
5	−1	6	0.1	0.0	−0.73	0.84

derived from the constituent elements of Table 1. In all cases shown the R_{11} element was variable. In sets 1, 2, 3, the α_M limit was penalized, and in sets 4 and 5 another penalty was placed on R_{11} to account for the $0° \leqq \alpha$ lower limit. The dramatic effect of the R_{11} element on the terminal error performance can be seen from comparison of the results for sets 2 and 5 for variable Q, and from comparison of sets 3 and 4 for constant Q.

The Q Matrix

The R matrix was the most critical choice for the problem considered since the R_{11} element could be selected to avoid

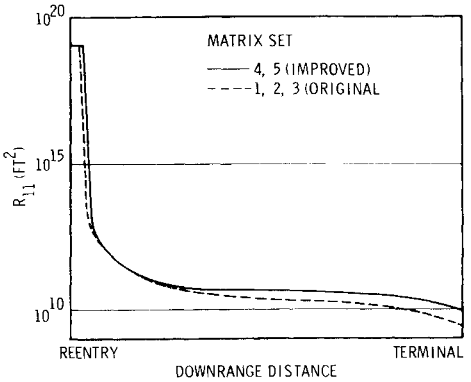

Fig. 9 Weighting matrix element R_{11} vs downrange distance.

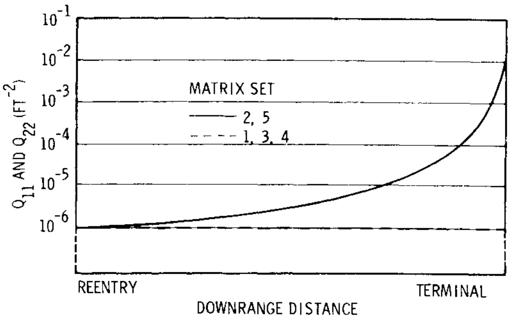

Fig. 10 Weighting matrix elements Q_{11} and Q_{22} vs downrange distance.

nonlinear behavior during maneuvering. The Q matrix reflects a penalty on deviations from the nominal trajectory on route. The Q_{11} and Q_{22} elements were tried both as constants, and as variables. The variable elements were derived from allowing the constituents δY_M and δX_M to go from 1000 ft to 10 ft linearly with the independent variable X, reflecting a greater penalty on deviations from the nominal trajectory as the terminal point is approached. The Q_{11} and Q_{22} histories are shown in Fig. 10.

The effect of variable Q on the terminal error performance is observed in Table 2 by comparison of set 1 with set 2 before the R matrix was improved. Note that the terminal errors are worse.

After the R refinement, however, the variable Q improved the terminal performance as seen by comparing set 4 with set 5. This is true even though there was a reduction in the penalty on the P_f matrix.

The P_f Matrix

This matrix reflects control over the terminal error itself, and large penalties on P_f cause large values of gain near the terminal point. The effect of increasing this penalty on the terminal errors is shown in Table 2 by comparing sets 1 and 3, in which both sets have constant Q and the variable R_{11} that was first chosen. A small reduction in terminal position error is seen.

Recommended Iteration Process for this Problem

This procedure is by no means recommended as a general one, but if a problem similar to this one were to be analyzed, the following procedures for determining R, Q, P_f might help as a guideline to an orderly choice of these weighting matrices. This process emphasizes the nominal trajectory following quality which was important for this study.

1) Start the weighting matrix selection process with P_f and constant Q, selected according to the rule of thumb. The

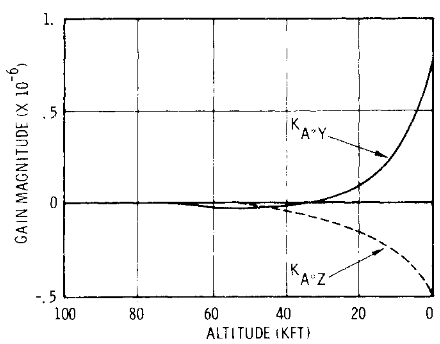

Fig. 11 Optimal feedback gains K_{A^*Y} and K_{A^*Z}; weighting matrix set 5.

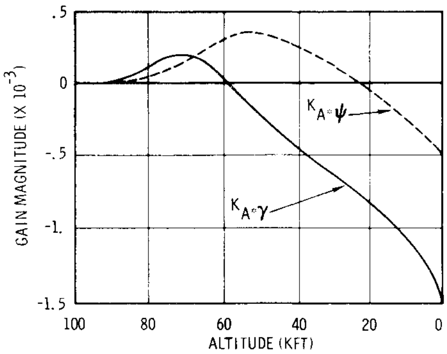

Fig. 12 Optimal feedback gains $K_{A*\gamma}$ and $K_{A*\psi}$; weighting matrix set 5.

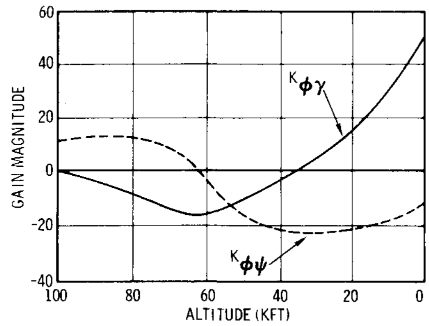

Fig. 14 Optimal feedback gains $K_{\phi\gamma}$ and $K_{\phi\psi}$; weighting matrix set 5.

maximum allowable errors used to define P and Q should not be chosen independently of each other. They must reflect the relative amplitude of oscillation of the state vector components when the uncompensated system is excited by a disturbance. A variable R should be used that reflects the actual inequality control constraints along the nominal trajectory.

2) Further improvement, if required, can be obtained by the use of a variable Q, for instance by increasing the penalty as the vehicle gets closer to the desired terminal point. In this case start with $P_f = 0$.

3) Finally, when Q is about right, further improvement in terminal error can be obtained by using $P_f \neq 0$, such that $P_{f_{ii}} \geqq Q_{ii}(t_f)$.

Optimal Gains for Weighting Matrix Set 5

The optimal gains that were calculated using weighting matrix set 5 are shown in Figs. 11–14. The usual tendency is seen for the gains to increase as the desired terminal point is approached. At exactly the terminal point, defined by zero altitude, the gains have a sudden decrease to very small values. In fact, at this terminal point the four-position dependent gains K_{A*Y}, K_{A*Z}, $K_{\phi Y}$, $K_{\phi Z}$ are identically zero. This is due to the form of P_f and G for this particular problem, and can be shown by expansion of $K_f = R^{-1}G^TP_f$.

Guidance Law Evaluation

The terminal error performance for $\pm 10\%$ variations in density (ρ), aerodynamic lift (C_L), and drag (C_D) is shown in Table 3, all based on the optimal gains derived from weight-matrix set 5. These results are from a 3-DOF nonlinear simulation and are referenced to the nominal condition. Terminal errors for initial conditions of ± 1000 ft in altitude (Z_o) and ± 1000 fps in velocity magnitude (V_o) are given in Table 4 The same method was applied to other trajectories with comparable success to the one discussed in the paper. In addition, the eight gains were fit with straight line segments requiring a total of 50 points for computer storage of the gains, as contrasted with the 640 points that resulted from the optimization. The $+10\%$ C_D off-nominal condition was then simulated, with a resulting slight, but negligible increase in terminal error.

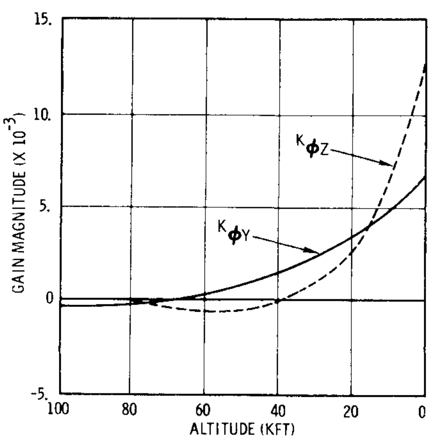

Fig. 13 Optimal feedback gains $K_{\phi Y}$ and $K_{\phi Z}$; weighting matrix set 5.

Table 3 Terminal error performance in off-nominal conditions[a]

Off-nominal condition	ΔX_f (ft)	ΔY_f (ft)	$\Delta\gamma_f$ (deg)	$\Delta\psi_f$ (deg)	ΔMach$_f$	Δt_f (sec)
-10% ρ	4	-11	0.0	0.1	0.24	-0.05
$+10\%$ ρ	2	-2	0.0	0.0	-0.27	0.10
-10% C_L	1	-4	0.0	0.1	0.00	-0.02
$+10\%$ C_L	-1	4	0.0	-0.2	-0.01	0.03
-10% C_D	12	-25	-1.4	-0.3	0.75	-0.59
$+10\%$ C_D	-1	6	0.1	0.0	-0.73	0.84

[a] 3-DOF nonlinear simulation results.

Table 4 Terminal errors for initial condition perturbations[a]

Initial condition error	ΔX_f (ft)	ΔY_f (ft)	$\Delta\gamma_f$ (deg)	$\Delta\psi_f$ (deg)	ΔMach$_f$	Δt_f (sec)
$+1000$ ft Z_o	8	-19	0.0	0.0	0.03	-0.08
-1000 ft Z_o	4	-9	0.0	0.0	-0.05	0.12
$+1000$ fps V_o	7	-17	0.0	0.1	0.30	-0.82
-1000 fps V_o	7	-12	0.0	0.1	-0.30	0.89

[a] 3-DOF nonlinear simulation results.

Conclusions

The over-all conclusion based on these results is that the linear optimal guidance as described in this paper, which includes the four-state dynamics for the perturbation dynamic model, is a viable scheme for aerodynamically-controlled re-entry vehicles as described. High accuracy for both path following throughout the trajectory and for terminal errors can be obtained for large initial condition perturbations and for large differences in density and lift and drag coefficients. Also, a procedure for determining the weighting matrices is proposed as a guideline for problems similar to this one.

References

[1] Hoffman, W. C., Zvara, J., and Bryson, A. E., Jr., "A Landing Approach Guidance Scheme for Unpowered Lifting Vehicles," *Journal of Spacecraft and Rockets*, Vol. 7, No. 2, Feb. 1970, pp. 196–202.

[2] Duiven, E. M., "Quadratic Cost-Re-Entry Guidance Laws," Internal Memo 2-5482-0100-020, Dec. 1969, Aerospace Group, Boeing Co., Seattle, Wash.

[3] Kovatch, G., "Optimal Guidance and Control Synthesis for Maneuverable Lifting Space Vehicles," *Transactions of the 9th Symposium on Ballistic Missile and Space Technology*, Vol. 1, Air Force Command, San Diego, Calif., 1964, pp. 327–379.

[4] Glover, L. A. and Hagan, J. C., "The Motion of Ballistic Missiles," TG1164, July 1971, The Johns Hopkins University, Applied Physics Lab., Baltimore, Md.

[5] White, J. S. and Lee, H. Q., "Users Manual for the Variable Dimension Automatic Synthesis Program (VASP)," TM X-2417, Oct. 1971, NASA.

[6] Anderson, B. D. O. and Moore, J. B., *Linear Optimal Control*, Prentice-Hall, Englewood Cliffs, N.J., 1971.

[7] Bryson, A. E. and Ho, H. C., *Applied Optimal Control*, Blaisdell, Waltham, Mass., 1969.

[8] Kwakernaak, H. and Sivan, R., *Linear Optimal Control Systems*, Wiley, New York, 1972.

OCTOBER 1974 AIAA JOURNAL VOL. 12, NO. 10

A New Method of Solution of the Eigenvalue Problem for Gyroscopic Systems

LEONARD MEIROVITCH*
Virginia Polytechnic Institute and State University, Blacksburg, Va.

This paper is concerned with the motion characteristics of gyroscopic systems described by $2n$ first-order ordinary differential equations defined by two real nonsingular matrices, one symmetric and one skew symmetric. The equations describe the motion of a spinning body containing elastic parts. Taking advantage of the special nature of the problem, a new method of solution of the associated eigenvalue problem is developed, whereby the eigenvalue problem is transformed into one in terms of two real symmetric matrices. A basic new concept is introduced in the form of a state vector that includes the rotational motion of the structure as a whole and the elastic motion relative to the rotating frame. Orthogonality relations and an expansion theorem are developed in terms of such eigenvectors. As an illustration of the method, the natural frequencies and natural modes of a spinning spacecraft containing elastic parts are calculated.

Introduction

THE theory for the eigenvalue problem for nonspinning systems with elastic restoring forces is well developed. By comparison, the eigenvalue problem for spinning systems containing elastic parts has received very little attention. Such systems can be defined in terms of two matrices, one symmetric and one skew symmetric, and belong to the general class of *gyroscopic systems*. With the advent of spinning spacecraft, the eigenvalue problem associated with gyroscopic systems has gained increasing importance, although work on the subject remains scant.

The problem of gyroscopic systems is mentioned by Frazer, Duncan, and Collar[1] in conjunction with Lagrange's equations for systems referred to rotating axes, but the discussion does not go beyond the formulation of the problem. Lancaster[2] points out that the eigenvalues of an undamped gyroscopic system are pure imaginary complex conjugates, and that the associated eigenvectors are also complex conjugates, but presents no special algorithm for the solution of the eigenvalue problem other than the general ones. The problem of a damped gyroscopic system, simulating a spinning satellite containing elastic parts, was discussed by Meirovitch and Nelson.[3] Reference 3 used a Rayleigh-Ritz approach to discretize continuous elastic members. The eigenvalues of the complete rotational system were obtained by solving the characteristic equation numerically, but no attempt was made to develop general methods of solution. The equations of motion for a complex gyroscopic system were derived by Likins.[4] Reference 4 proposes a solution in terms of the eigenvectors for the elastic displacements alone, with the terms due to the rotational motion of the spacecraft being regarded as external excitations. Consistent with this approach, Ref. 4 provides a brief survey of possible ways of solving the eigenvalue problem associated with nonrotating damped structures, but no numerical example illustrating the approach is presented. Using the approach of Ref. 4, Patel and Seltzer[5] propose a computer program to solve the eigenvalue problem associated with the elastic displacements alone. The case of constant angular velocity receives special attention. Following the same line of thought as in Refs. 4 and 5, Gupta[6,7] also concerns himself with an eigenvalue problem for elastic deformations alone. References 6 and 7 avoid the question of rotational degrees of freedom entirely by considering mathematical models consisting of elastic structures spinning with constant angular velocity about an axis fixed in space. These are computationally oriented papers in which the author proposes an algorithm that takes advantage of the fact that the eigenvalue problem is defined by highly banded matrices, but not explicitly of the fact that one matrix is symmetric and the other is skew symmetric. Although the mathematical models are intended to represent spinning space structures, the fact that the

Received January 7, 1974; revision received May 17, 1974. This paper was presented at the Seventh U.S. National Congress of Applied Mechanics, Boulder, Colo., June 3–7, 1974.

Index categories: Spacecraft Attitude Dynamics and Control; Structural Dynamic Analysis.

* Professor, Department of Engineering Science and Mechanics. Associate Fellow AIAA.